Sedimentary Geology, 71 (1991) 151–175
Elsevier Science Publishers B.V., Amsterdam

Sedimentation and palaeoenvironment in crater lake Barombi Mbo, Cameroon, during the last 25,000 years

Pierre Giresse [a], Jean Maley [b] and Kerry Kelts [c,*]

[a] *Laboratoire de Recherches de Sédimentologie Marine, Université de Perpignan 66860 Cedex, France*
[b] *Laboratoire de Palynologie, ORSTOM and CNRS USTL, Montpellier 34095 Cedex 05, France*
[c] *Geology Section, Swiss Federal Institute of Water Resources (EAWAG/ETH), CH 8600 Dübendorf, Switzerland*

Received February 14, 1990; revised version accepted January 30, 1991

ABSTRACT

Giresse, P., Maley, J. and Kelts, K., 1991. Sedimentation and palaeoenvironment in crater lake Barombi Mbo, Cameroon, during the last 25,000 years. Sediment. Geol., 71: 151–175.

Lake Barombi Mbo is situated in a maar crater of the Cameroon volcanic chain. Sediment cores were recovered with a Livingstone corer. This paper presents data on core BM6, 23.5 m long, from a water depth of 110 m. The sediments are mainly organic matter-rich clays (5 to 10% total organic carbon) showing alternating brown and yellowish horizontal laminae on a cm-scale. The lower part of a couplet (basal sublamina) is rich in siliciclastic (quartz, mica) grains, sponge spicules and documents the deposition of flood detritus. The upper unit (upper sublamina) is composed of grey to bluish clay which becomes green toward the top with frequently yellow, layered concretions of siderite. It corresponds to quiet conditions with settling of fine clayey particles from suspension. The overall recurrence rate of these laminae is about 15 years. This frequency is similar to present-day large flood events in this intertropical zone. From 14,000 to 20,000 yrs BP, the sediment accumulation rate was quite low (15–30 g cm^{-2} 10^{-3} yrs). With less abundant precipitation, pedogenic clay formed from mica-family minerals. From 12,000 yrs BP throughout the Holocene, the rate of accumulation increased (> 40 g cm^{-2} 10^{-3} yrs) and increasing precipitation favoured the pedogenic formation of kaolinites. Turbidity currents became less important to the overall sedimentation. Plankton production remained low, documented by organic matter which is more of the exinite than the alginite type. Siderite concretions occur as early diagenetic products, possibly related to alkalinity in anoxic waters at the sediment–water interface which limited the formation of Fe^{3+}.

Thin ash layers occur between 11.5 and 18 m depth in core BM6, bearing witness to several volcanic events during the Late Quaternary. Sediments are disturbed below 21 m with folded laminations and inverse ages. These probably result from a slump glide of lower slope sediment but could also signal a possible gas event.

Introduction

In contrast to the rift zone of East Africa, West Africa lacks large, permanent deep lakes which can be cored to obtain a continuous reference section of Quaternary palaeoenvironment changes. One of the first subsaharan sites tested has been the meteorite crater lake of Bosumtwi, Ghana, situated within the forest belt. Talbot et al. (1984) and Maley (1989) documented a ca. 30,000 years history of palaeoclimate and vegetation evolution with aridity in concert with high-latitude glaciation.

Numerous lakes of volcanic origin dot the Cameroon Line, a volcanic ridge extending from Mt. Cameroon to the Adamaoua Massif (Gèze, 1943; Cornaccia and Dars, 1983; Fitton and Dunlop, 1985). These lakes provide a unique opportunity for a transect of Late Quaternary coring sites which cross the current climate–vegetation zones of subsaharan Africa: rain forest, forest–savanna contact zone and savanna. During times

* Present address: Director, Limnological Research Center, Pillsbury Hall, Univ. Minnesota, Minneapolis, MN 55455, USA.

0037-0738/90/$03.50

of cooler climates, mountain biotopes migrated to lower altitudes, replacing more or less lowland-forests, which survived in a series of forest refuges along the Gabon–Cameroon belt (Maley, 1987, 1989).

A seismic reconnaissance expedition in January 1985 selected the first transect site at Lake Barombi Mbo, near the village of Kumba, within the dense, lowland rain-forest area of Western Cameroon (Fig. 1).

Although several of the crater lakes surveyed show effects of recent volcanism, others appear to have remained dormant over several tens of million years. Catastrophic expulsion of CO_2 from two crater lakes of West Cameroon (Lake Nyos and Lake Monoum; Kling et al., 1987; Sigurdsson et al., 1987; and others) has focused attention on such hazards in maar crater lakes. Controversy continues on the exact causes of such catastrophes. Long core records from Barombi Mbo may provide one sediment tool to observe Quaternary evidence of comparable events.

Geographic and geologic setting of Lake Barombi Mbo

Lake Barombi Mbo sits at 301 m elevation, at 4°39′45″N 9°24′15″E and about 60 km NNE of the 4000 m high active Mt. Cameroon stratovolcano.

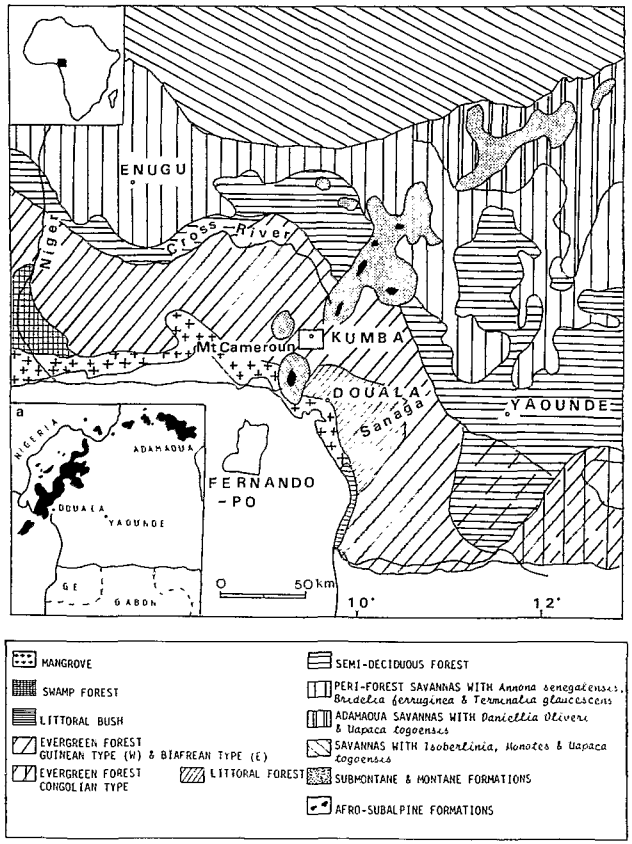

Fig. 1. Index map of west equatorial Africa with the distribution of vegetation zones in the areas surrounding Lake Barombi Mbo. Location within Africa. Volcanic ridge of the Cameroon Line (a).

The modern climate of the west Cameroon forest is of the equatorial type (Letouzey, 1968; Suchel, 1972, 1988). Beginning in the months March–April, moisture is transported northward by unstable monsoon fronts. In June, rains increase and cloud cover thickens. Solar radiation decreases as a consequence. In October, the monsoon shifts southward, accompanied by masses of dry air pushed from the north by the hazy Harmattan wind. December through February is the driest period of the year. Average annual rainfall ranges from 3,000 to 4,000 mm, with significant local variability, particularly around Mt. Cameroun. For example, the station of Debundscha, facing west toward the ocean at the foot of Mt. Cameroon, receives an average of 10 m per year, whereas a station on the NE foot of Mt. Cameroon receives less than 2,000 mm per year due to the rain shadow effect of the massive volcano (Suchel, 1972, 1988). Within this lowland rain-forest region the dry season lasts only through December and January or February, when rainfall is about 50 mm/month or less. The closest meteo-station to Lake Barombi Mbo is near Kumba (Figs. 1 and 3) where an average 2365 mm per year is recorded, mainly during March to October. This pattern should be reflected in the sediments of the lake by seasonal couplets.

The main features of the vegetation (Fig. 2) for a radius of 10–20 km around Barombi Mbo (Richards, 1963; Letouzey, 1968, 1985) are: (1) the dominance of evergreen forest characterized by an abundance of leguminous trees; (2) the presence of islands of semi-deciduous forest within the evergreen forest; (3) another important feature is a few hundred hectares of relict savanna surviving on the northern foothills of Mt. Cameroun, due to the rain shadow effect of the mountain.

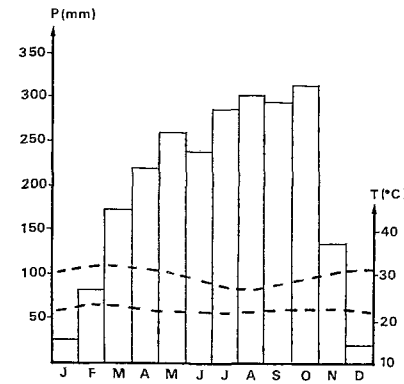

Fig. 2. Histogram of the average monthly precipitation at the Kumba station (from Suchel, 1972).

The lake formed in a basin composed of two intersecting explosion calderas with quite youthful characteristics. From west to east, these maars are punched through the Upper Black Series of basaltic tuffs and lava flows and through the gneissic substratum basement (Gèze, 1943; Dumort, 1968). A basaltic flow on the NE shore of the lake has been dated by six K/Ar measurements giving an age of ca. 1 Ma year (Maley et al., 1990; Cornen et al., in prep.). This age is consistent with the present day morphology of the Barombi Mbo compared with nearby craters along the chain, such as the lake Nyos crater dated between 5,000 and 400 years BP (Lockwood and Rubin, 1989). The crystalline basement outcrops in the western part of the drainage basin (Maley et al., 1990). Subaerial flats of the western crater are covered by a 2–3 m thick fersialitic soil (observation by G. Bocquier, ORSTOM). Elsewhere, such as to the north of Barombi village (Fig. 3), the soil is hydromorphic, i.e., it comprises a bluish-gray gley with some rusty coloured pockets up to 50 cm thick. Steep slopes have a thin cover of poorly developed soils or are denuded.

Morphology and hydrology of Lake Barombi Mbo

With a diameter of about 2 km and a maximum depth of 110 m Barombi Mbo is the largest of the lakes along the Cameroon Line. The lake surface is at an altitude of 301 m. The general bathymetry describes a bowl with a broad flat basinal plain, and narrow marginal apron rising abruptly along steep slopes to a narrow littoral shelf (Fig. 3). The catchment lies mostly on the western side and is drained by a little perennial stream called Toh Mbonk which has built a steep delta cone prograding several hundred metres towards the lake center (Figs. 3 and 4). The drainage basin is not limited to the steep inner wall of the crater rim, but also includes most of the emergent surface of

a second boxed caldera. Together they provide about 8 km^2 catchment which is less than double the surface of the lake.

The level of the lake is stabilized by a natural spillover (reinforced ca. 20 years ago by a small concrete dam) which cut down a gorge in the rim, over 100 m into the southeastern crater wall. Hydrology and limnology were studied by Kling (1987, 1988) who noted that the lake is oligotrophic, as is the case with many Cameroonian lakes. The water is very dilute but is stratified, with a conductivity of 46 μS at the surface and 110 μS at depth. This low total dissolved solids concentration increases slightly during the dry season. Waters are of a bicarbonate type with minor sulfate. Principal cations are calcium, magnesium, and potassium. The surface pH is near neutral (7.14–7.52) and becomes more acidic with depth showing a pH of 6.42–6.60 at 100 m. Several ions show increased concentration in the hypolimnion including calcium and silica. These cause the doubling in conductivity along with bicarbonate values 1.5–2 times higher than surface values. The water body attains stable stratification at least during part of the year (see Table 1). The water is extremely clear with a Secchi disk mean transparency of 11 m, or one of the highest in the region. Seasonal and annual variability in dissolved solids concentration is limited. There is less than 8% for silica and 15 to 20% for the anion concentrations. The relative percentage among the elements changes little, suggesting that calcite does not precipitate.

The surface water temperature follows a narrowly defined annual cycle linked to the air temperature and the insolation. It ranges from 28.65°C

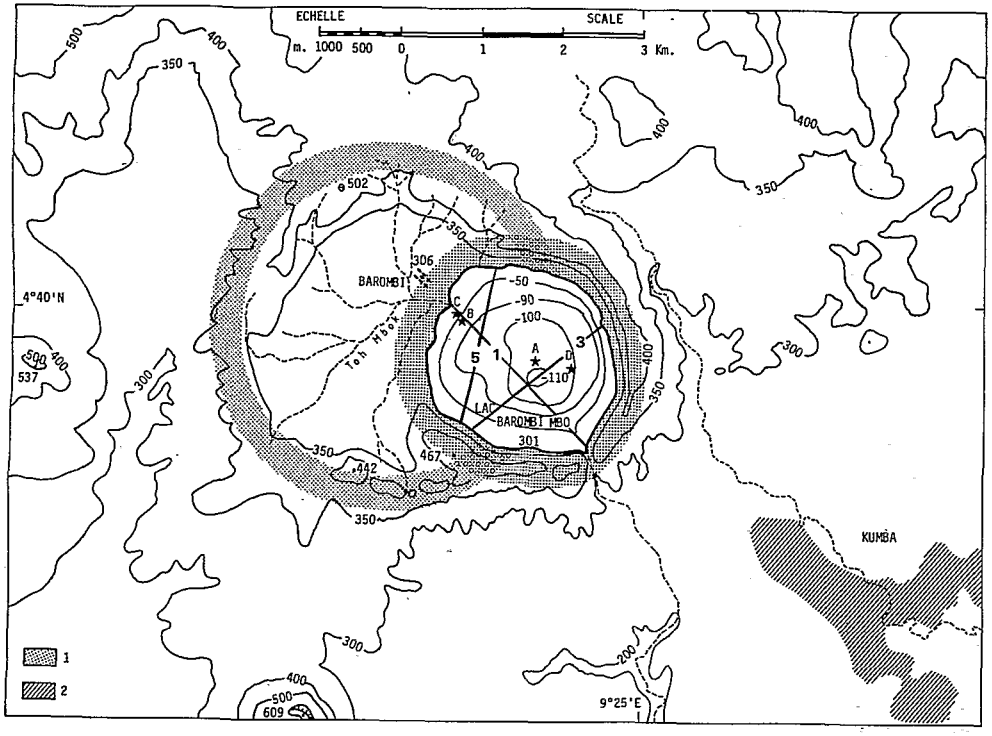

Fig. 3. Simplified bathymetric map of Lake Barombi Mbo after Hassert, 1912. The lines *1* through *5* show the location of seismic survey transects and the stations *A*, *B*, *C* and *D* are coring sites. The inner circle is the lake level near today and the outer rings indicate the drainage basin of the lake and the rim position of the two boxed craters.

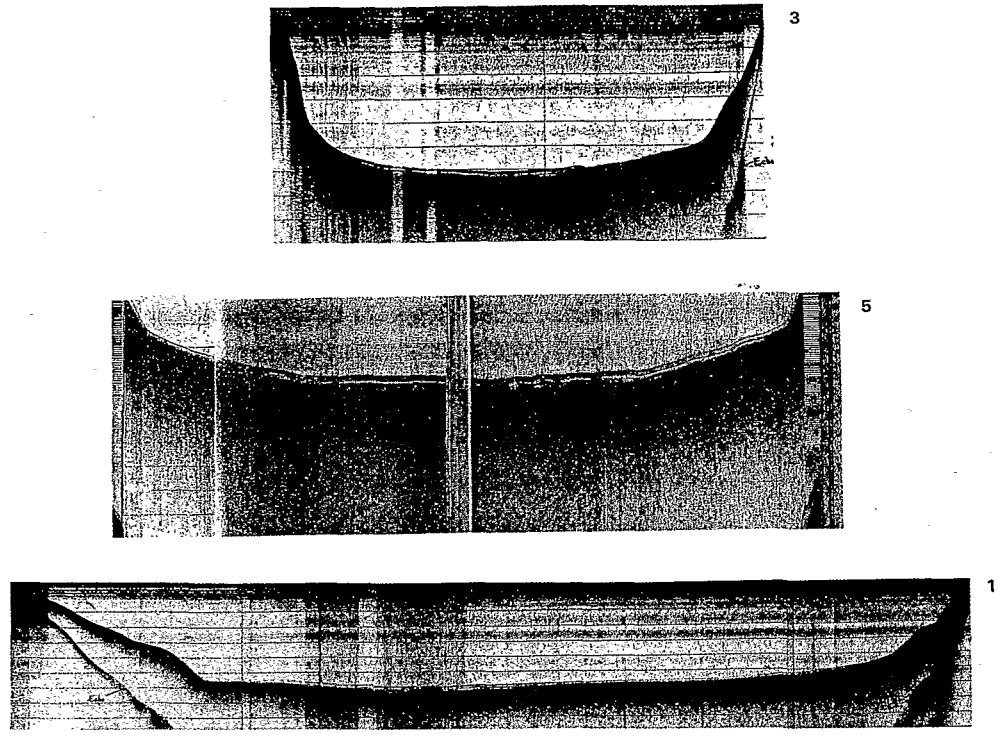

Fig. 4. An example of a high-resolution 3.5 kHz seismic profile showing bathymetry of Lake Barombi Mbo, profile 1. Note that penetration is only a few metres down to an irregular surface interpreted as a slump deposit (*1*, *3*, *5*: cf. Fig. 3).

in February to 26.65°C in September (Fig. 5). The thermocline rises from −38.5 m in February to −29 m in April. In spite of these figures, the water column stability appears greater in Barombi Mbo than in many other tropical lakes (Kling, 1987, 1988). Stability becomes weakest in August–September (about 3000 J m^{-2}) but with no indication of a complete turnover. The thickness of the metalimnion is from −15 to −25 m and defines the transition from the mixed zone to the anoxic water mass.

Productivity of plankton biomass is low. Eleven endemic species of cichlid fish (Green et al., 1973) depend on Rotifera, Cladocera, and Copepoda

TABLE 1

Seasonal variability in the water chemistry of Lake Barombi Mbo (after Kling, 1987)

	Depth (m)	pH	Cond	HCO_3	Cl	SO_4	Ca	Mg	Na	K	Fe	Al	SiO_2
End of dry season 1985	0	7.52	49.1	24.2	0.65	0.20	2.81	2.49	2.37	1.05	0.01	0.37	12.29
	100	6.47	80.2	32.5	0.80	0.02	7.49	2.55	2.65	1.17	0.04	0.42	16.11
End of wet season 1985	0	7.14	49	26.5	0.64	0.20	2.65	2.53	2.46	1.02	0.02	0.38	12.18
	100	6.42	101	34.6	–	–	3.19	2.58	2.52	1.19	0.13	0.43	15.90

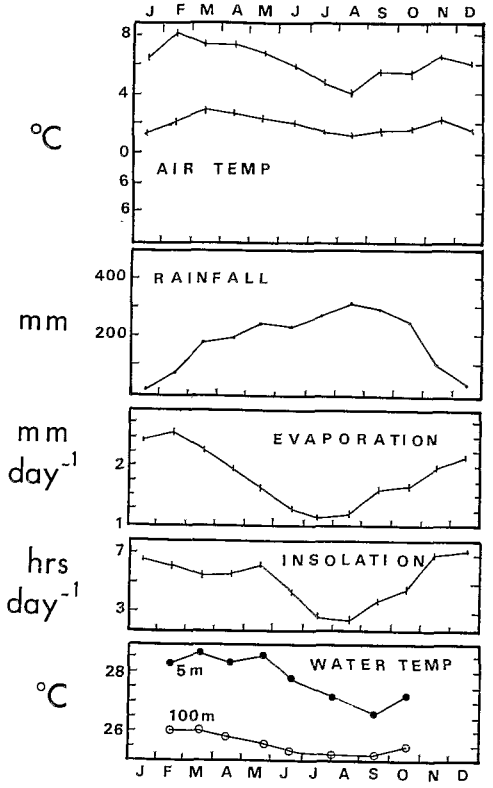

Fig. 5. Weather data from the Barombi-Kang meteorologic station, 5 km south of Barombi Mbo; rainfall means are monthly totals for the period 1968–1985; air temperatures are averages for 4 years; insolation averaged for 24 years (after Kling, 1987).

(Kling, 1987). Siliceous sponges colonize benthic areas of the platform shelves. Gastropods (*Potadoma freethi*) were observed in minor abundance along the Toh Mbonk stream (identification by J. Monteillet, Yaoundé).

Field methodology. Coring operations were conducted by Prof. D.A. Livingstone from Duke University, USA, with the help of G.W. Kling, C. Stager, J. Maley, P. Nduni and A. Zogning. Operations included the construction of a catamaran platform, 6×6 m^2 with tripod and winch, anchored in the centre of the lake. The modified Livingstone corer uses a piston, and steel core tubes 3 m long and 56 mm in interior diameter. Six cores (BM1 to BM6) ranging from 5.6 to 23.5 m long were obtained from point A in 110 m water (Fig. 3). Three other cores (BM7 to BM9) were recovered from points B and C in 30 and 60 m water across the delta of Toh Mbonk. This paper is devoted mainly to the longest core, BM6 (23.50 m).

The chronology has been determined from radiocarbon dates on bulk sediment samples and separated organic fractions (M. Fournier, ORSTOM Bondy, France). The chronologic framework was also compared to the scale established by palaeomagnetism (Thouveny and Williamson, 1988).

The sediments are laminated throughout core BM6 on a sub-centimetre scale, but sample intervals were on the order of every 10 cm for lithologic logging. The intervals were varied depending on layer thickness. In addition, characteristic lamination sets were sampled in detail (sub-centimetre scale) for smear slides and mineralogy.

After water content determinations, each sample was washed at 50 microns. The sand fraction was examined by stereoscope, and the rest by X-ray diffraction (XRD) using a copper source. Mineralogy was determined by XRD on bulk samples and every third oriented clay sample. Grain-size analyses on every third sample were carried out by Sedigraph 5100, with the > 50-micron fraction added to the cumulative curve; samples were placed in a 0.1 vol.% sodium hexametaphosphate solution, then in a 30 vol.% H_2O_2 solution; disaggregation was achieved by the suspension being placed on a shaking table and then in an ultrasonic bath. Organic carbon (coulometer) was determined on every third sample, with nitrogen (Kjeldahl method). Selected samples were impregnated and the microlaminations studied on thin sections.

Results

Sediments and structures

Although this study mainly focuses on the long core BM6, we give a brief overview below of the core lithologies from those sites transecting the delta (point C) and on the delta slope (point B) (Fig. 3).

Core BM9 from −32 m penetrated approximately 8 m of sediment. Sediments are dark grey, rather homogeneous, uniform silty-muds intercalated with several brownish layers. This relatively coarse-grained mud shows no evidence of laminations but on the other hand is very rich in land-derived organic debris, in particular millimetre- to centimetre-size fragments of palm nuts.

The cores BM7 and BM8 at −59m on the delta slope have lengths of 2.5 m and 10 m, respectively. Sediments are dark grey and noticeably finer-grained than those at −32 m, but also homogeneous. This documents a basinward decrease in grain size from fine muddy silt to very fine silty clay. Flakes of fine-grained muscovite are almost ubiquitous and concentrated in some silt layers. Fragments of wood and leaves are concentrated at several levels, but these sediments display no laminations or yellow siderite concretions: only irregular-graded bedding can be observed. In Fig. 3, point D is close to the transition from slope to basin clay. The limit of the extension of the deeper laminated sediments is generally near −90 m, as has been verified by a series of short surface cores (M. Pourchet et al., in prep.).

Core BM6 at −110 m displays conspicuous laminations throughout its length of 23.5 m. For the most part the sediments are dark brown to greenish gray. Laminations which form frequently a composite microsequence vary in thickness from less than 1 mm to 3 or 4 cm. These microsequences commonly present: (1) a thin brown to black lower sublamina consisting of fine-grained quartz and flakes of mica; fragments of microscopic organic debris are scattered within; and (2) an upper sublamina mainly blue to greenish clay which near the top commonly has tiny concretions of siderite; the colour of the top of each of these microsequences is determined by the concentration of siderite.

The uniform character of sedimentation in core BM6 is perturbed by the following two separate processes.

(1) Frequent influxes of millimetre- to centimetre-layers of volcanic ash. Composition of these layers is rather uniform, comprising basaltic clasts (Cornen et al., in prep.) characterized by microlaminae of plagioclase feldspar, with labradorite composition, and by olivine. The excellent state of preservation of these pyroclasts indicates that they were completely cooled before direct sedimentation in the lake or indirectly from rain washing in the catchment and rapid runoff. The pyroclastic laminae are interstratified in the sediments mainly between −17 and −11 m. However, a stereo binocular examination shows that traces of pyroclastite persist up to the top of the core, with particular recurrences around −3.5 and −2.5 m (Fig. 6) (Cornen et al., in prep.). Pyroclastic laminae are commonly accompanied by small grains of magnetite.

(2) The core displays significant slumping structures near the base with spectacular slump folds between −23.4 and −.21 m. Laminated deposits are turned to the vertical with a kink near 23.4 m (Figs. 6 and 7). Two others zones with distinctly folded laminae occur around −19.6 m and at −18.6 m. We also note a common convexity of beds around −4.6 m, −5.15 m, −6.80 m, −11.3 m to 11.5 m. These beds are generally related to zones with pyroclastics and are thus possibly due to deformation by coring operations. However, the zone beneath 18.5 m appears to be a single slump unit to the base of core BM6. The 3.5 kHz seismic profiling in this region provides further evidence of a major perturbed deposit at the base of the section.

Throughout the core there were no indications of bioturbation in any laminae.

Chronology

Radiocarbon measurements were mostly performed on the total (mineral + organic) carbon fraction of the sediment. For two zones near −10 m and at the base of the core, measurements were made on duplicate samples; one bulk and one with the organic matter fraction separated. The ages were 5–10% higher for samples of the organic-carbon fraction. These differences in average age may represent differences in the variable residence times of the organic material at horizon A2 of the soil profiles in the drainage basin and the carbon used to form the mineral siderite. The differences in age between the organic fragments and the bulk organic carbon may also be related

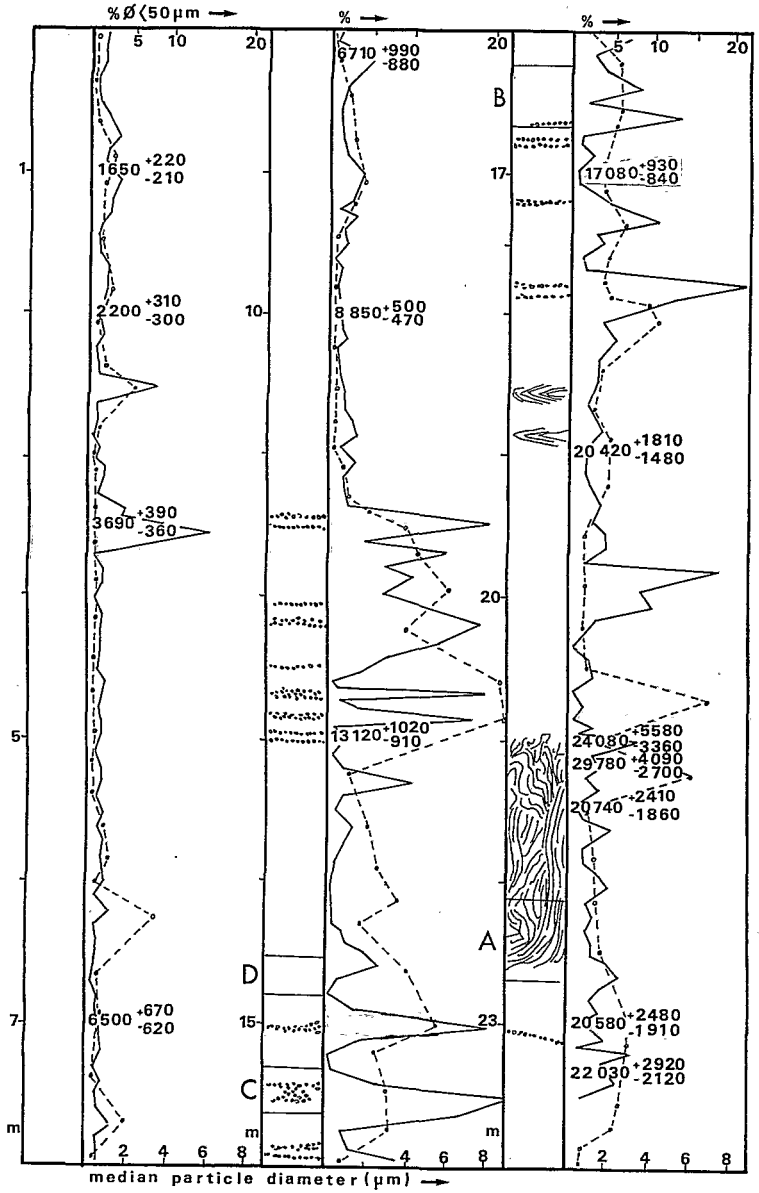

Fig. 6. Simplified lithologic log of core BM6 noting the position of laminae and layers of pyroclastites; zones with disturbed and faulted sedimentation; and the ages from radiocarbon dating. The curves to the right of the logs record the abundance of particles greater than 50 µm within the solid line and mean grain sizes within the dotted lines. The levels *A*, *B*, *C* and *D* refer to the photographs in Fig. 7 giving examples of sedimentary structures from core BM6.

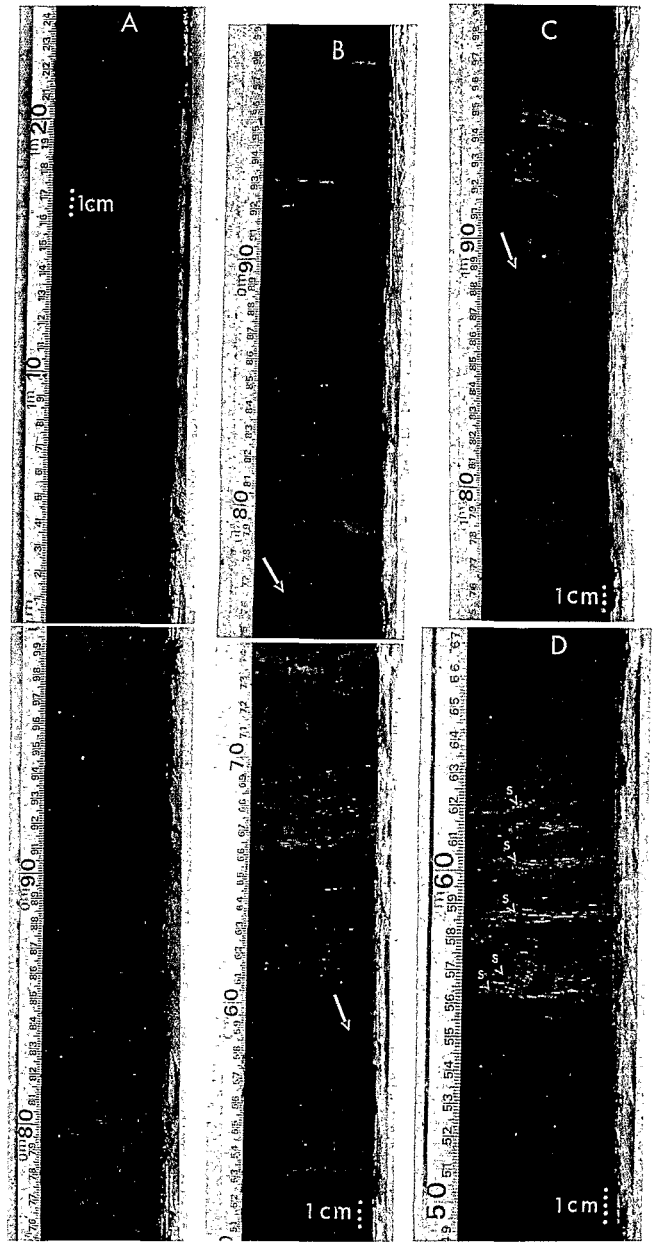

Fig. 7. A. Base of rhythmic laminae around −22.5 m with disturbance. B. Microsequence with well-defined brown laminae from around 18,000 years BP at −16.5 m; includes several millimetre-scale laminae of pyroclastic debris (white arrows). C. Centimetre-scale layer of pyroclastite interstratified at −15.5 m. D. More clay-rich laminae with presence of yellow concretions and thin laminae of siderite in the uppermost part (arrow).

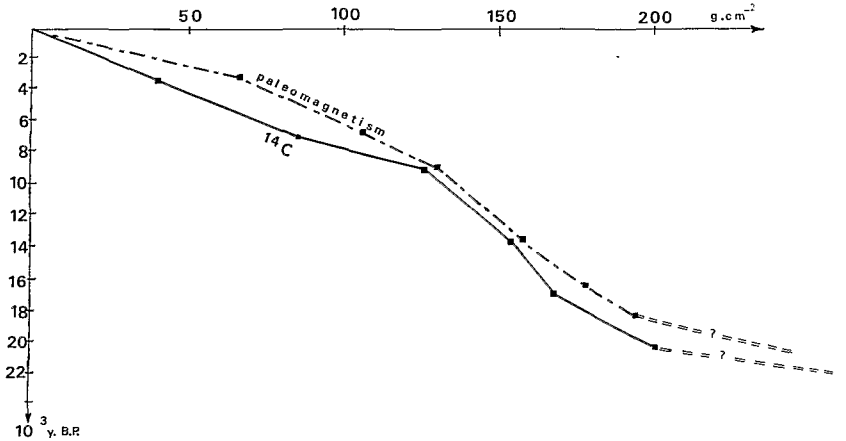

Fig. 8. Rates of accumulation of sediments in core BM6 comparing plots of radiocarbon dates and the peaks on secular palaeomagnetic curve (Thouveny and Williamson, 1988).

to post-depositional formation of humic acid within the sedimentary column as well as sideritic concretions.

The ages at the base of core BM6 range from 22,030 BP to 24,660 BP, depending on whether measurements are of total carbonate or organic fractions. However, the age sequence seems to be disturbed below 18.5 m in core BM6 so that we believe that the entire section from −18.5 m to −23.5 m represents a single slump event reversing some of the section, whereas other parts of the section appear to be deformed, but in stratigraphic continuity. Thus analyses below −18.5 m must be interpreted with great caution. Age dates of layers displaying extreme vertical deformation of the laminae are 24,080 BP to 29,780 BP.

The calculated accumulation rates on dry weight bases therefore appear to be between 13 and 46 g

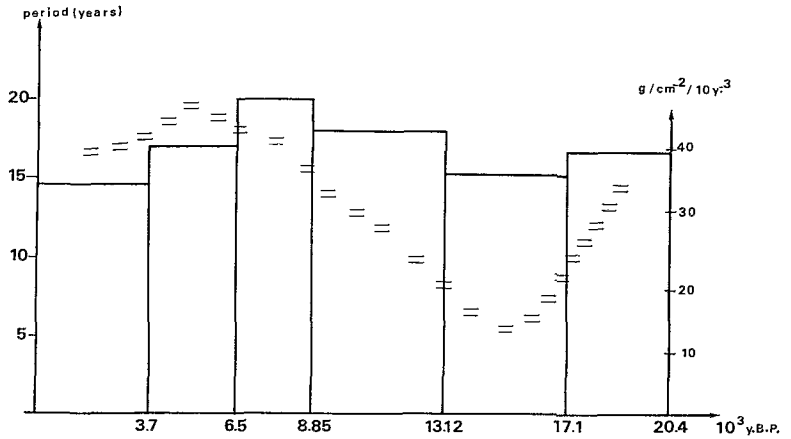

Fig. 9. Average repetition frequencies for laminae (histogram) as a function of the sedimentation rates (dash-line) for different periods in core BM6.

$cm^{-2}\ 10^{-3}$ yrs. These suggest an acceleration of sedimentation rates in the Holocene; the period with the lower sedimentation rates is between 17,080 BP and 13,120 BP (Fig. 8). Taking into account the disturbance of the sediments below −18.5 m, it is not possible to calculate an accumulation rate below the level of 20,420 BP. This suggests that the timing of the slumping was around 20,000 years ago.

Curves of secular palaeomagnetic variation (Thouveny and Williamson, 1988) provide an independent method for comparison with the sedimentation curves for the last 20,000 years. In comparison to the radiocarbon ages, the peaks on the palaeomagnetic secular variation curve appear to be systematically shifted toward younger ages (Fig. 8). This shift is also attributed mainly to the residence time of organic debris in drained basin soils. However, the palaeomagnetic secular variation curves of Thouveny and Williamson are difficult to apply in tropical equatorial Africa because the dating calibration of the non-dipole field-cells is far from well-established.

Microstructure of rhythmic laminations

The study of the most common and complete microsequences allows us to note the following ideal microsequence for the accumulation of a lamina.

(1) A sub-cm scale microsequence begins with a brown *lower sublamina* in which grain size and thickness covary. On a centimetre scale, one observes a significant concentration of quartz grains

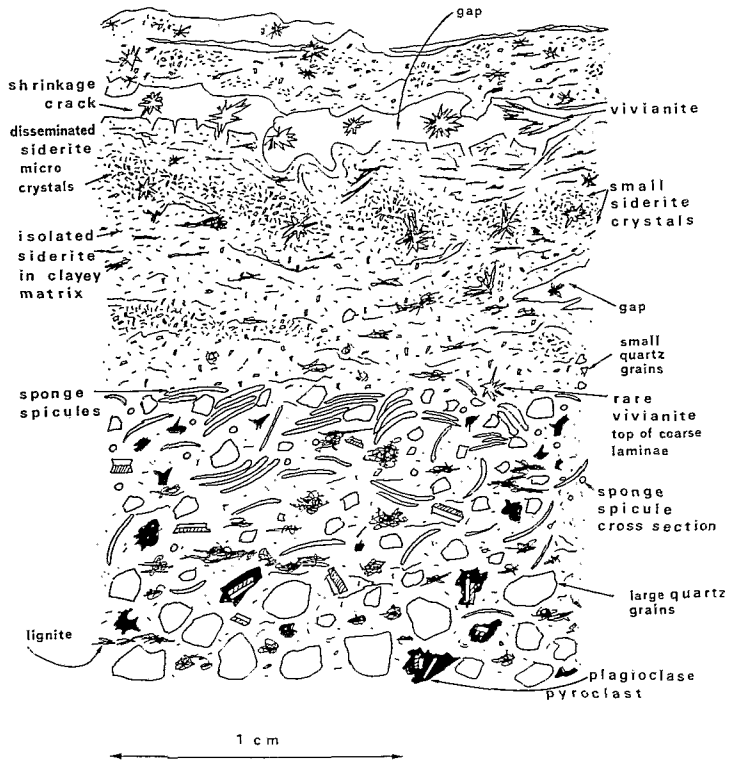

Fig. 10. Schematic sequence for a single idealized mini-rhythm. Lignitic debris, quartz grains, pyroclastic fragments with plagioclase laths, concentrations of sponge spicules, rare vivianite crystals in coarser layers, cross-section of sponge spicule, fine quartz silt, microcrystalline laminae of siderite, clay-rich, clotted-siderite crystals, siderite crystalites with faint halo of smaller crystal zones; larger vivianite crystals.

between 50 to 150 μm along the base. These are commonly associated with microlaths of plagioclase and fragments of pyroclasts with plagioclase phenocrysts or more rarely, grains of olivine, particularly in the layers before 10,000 BP. (Cornen et al., in prep.). Younger than 10,000 BP, the ferruginous organic sedimentary matrix is less abundant and encloses quartz silt grains (10 to 50 μm). Towards the upper half of the sublamina, the flakes of mica and the lignitic organic debris up to millimetre-size occur at the same intervals as concentrations of sponge spicules which can be extremely abundant (Figs. 10, 11 and 12b). The relative importance of ferruginous organic-matrix increases upward. We note that the brown lower sublamina which are coarsest and thickest, are the least-rich in sponge spicules. It is in this upper half that one finds some diatom frustules; most commonly between ca. 13,120 BP and 20,420 BP.

(2) *The upper sublamina* of one ideal sequence is dominated by clay and generally displays disseminated yellow prisms of siderite on the order of 5 μm in diameter. The concentrations of these grains increase toward the top and controls the colour changes in the deposit: grey, blue, then green. Siderite occurs in two geometric habits of concentrations. One habit is a very thin, less than one millimetre thick layer and more rarely as a sort of occluded distribution of microcrystals, more or less aligned along the bedding (Figs. 10 and

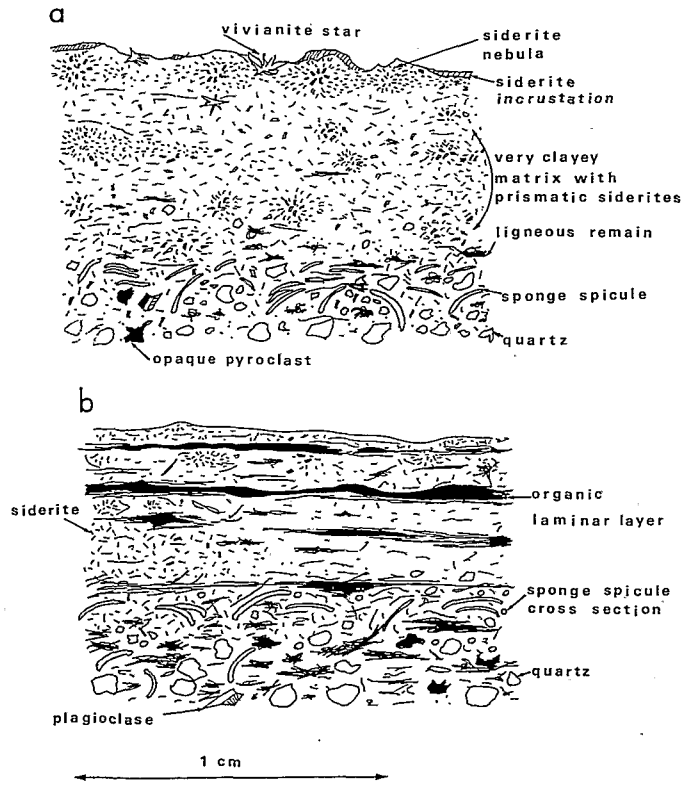

Fig. 11. Examples of microsequences from two typical lamination types. a. Sideritic clay lamination typical of the base of the Holocene section. Quartz grains, sponge spicules, lignitic organic debris, microprisms of siderite and a cap of concretionary siderite with some clotted zones and vivianite crystals. b. Brown lamina with organic-rich rhythmic microlamina typical of the zone near 17,000 years BP, plagioclase and quartz grains, rare sponge spicules, siderite microcrystals and microlaminae of organic-rich debris.

13a). In another more rare habit the crystals form bright yellow concretions: these are on average more common in the Pleistocene laminations than in those of the Holocene period. Fine-grained organic fragments are scattered within this upper sublamina, or are ordered along several interlayered microlaminae (Figs. 11b, 12d, 13a). Finally, toward the top of a microsequence, vivianite occurs as tabular crystals (to 20 μm), or in some cases as very small lensoid concretions which deform the original lamina (Fig. 13, b and c). Vivianite was observed immediately after opening the cores; however, its occurrence along fissures and cracks suggests that in some cases the vivianite also formed after the cores were taken (Fig. 14a).

The laminations from the first part of the Holocene section commonly lack quartz grains, in which case the individual lower brown sublamina are conspicuously rich in sponge spicules and especially in fragments of organic debris.

Laminae were counted directly after opening of the core. The frequency in core BM6 is inversed in relation to the rate of accumulation. We counted one set for each 15.2 years during the period 17,080 BP to 13,120 BP and one for each 19.9 years between 8,850 BP and 6,500 BP (Fig. 9). In general, laminae for which the repetition rate is less, are those with the thicker brown lower sublamina near the base of the core. We counted between 7 and 11 brown lower sublamina per metre between 20,420 and 13,120 BP.

Interlayering of dark organic microlaminae (flake-like) within the clayey upper sublamina (Fig. 11b) is a function of their thickness; in some cases, we count 10 to 15 of these microlaminae within an upper sublamina approximating the repetition of annual varves.

Grain size, mineralogy and geochemistry

The median grain size of the cored sediments is extremely fine. The values range around 2 μm, or generally about 1 μm for the Holocene and near 2 μm for the Pleistocene, with peaks up to 6 or 10 μm (Fig. 6).

Fluctuations of the median grain size are controlled by the presence or absence of sand fractions. Abundances of 20% or more of sand fractions coincide with the pyroclastic debris, or with coarser detrital grains, in particular quartz, which display dissolution etching related to pedogenesis. In some cases the fractions associated with quartz or pyroclastics show the effects of stream transport within the drainage basin. In some cases, grains of ferruginous pseudo-ooliths are a rare constituent of the sand fraction, but may represent 80 to 90% of this fraction in Holocene sediments where quartz and pyroclasts are rare. The grains of ferruginous pseudo-ooliths are composed of various proportions of iron and alumina silicates. Mineralogically, iron appears in an amorphous state or as siderite cement (Fig. 13). The alumino-silicate mineral appears to be poorly crystallized, or degraded kaolinite with a peak at 7Å on XRD.

The levels with abundant clayey sediment between 9,500 and 8,500 yrs BP, and between 6,000 and 3,000 yrs BP have median grain size of only 0.3 μm. The fraction below 0.3 μm was separated by ultra-centrifuging and analyzed by XRD. Crystallized alumino-silicates are rare while high organic carbon and iron contents were detected by chemical analysis.

Sedigraph cumulative sums look hyperbolic for most of the Holocene sediments, which suggests sedimentation by decanting from a uniform suspension in a calm environment. The addition of a sandy component changes the curve to sublogarithmic for several Pleistocene layers. There are no parabolic curves which would indicate significant transport by turbidity currents (Rivière, 1952; Kranck, 1984).

Mineralogy and geochemical logs

Figure 16 plots relative peak heights of silt–sand minerals recorded with uniform X-ray diffraction conditions as a useful overview of the variability of the principle constituents. Quartz is ubiquitous but in low abundances with irregular values in the Pleistocene levels and very weakly represented in the early part of the Holocene, increasing in the upper part. Opal which corresponds to sponge spicules, is uniformly distributed along the vertical and slightly more common in the clay-rich lamina of the Holocene. Siderite occurs in all samples and

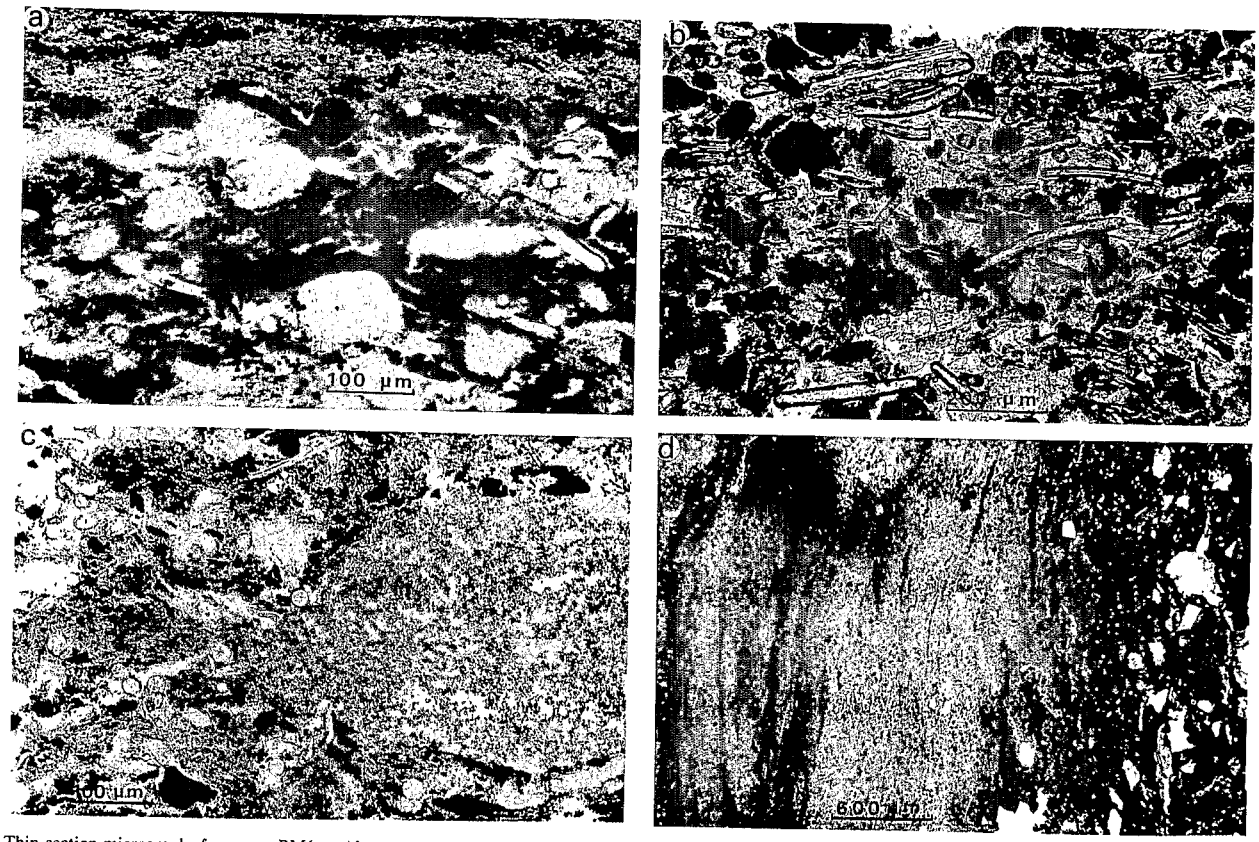

Fig. 12. Thin-section micrographs from core BM6. a. Abrupt transition from brown microlamina to zone of quartz and sponge spicules set into a ferro-organic matrix of the clay-rich lamina containing microcrystals of siderite (×160) (BM6-5; 77–73 cm). b. Brown lamina with abundant sponge spicules parallel to bedding and abundant organic debris (×100) (BM6-6; 31–35 cm). c. Post-depositional siderite microcrystals as clotted zone above or engulfing a sponge spicule to the right; these occur along the transition from a brown microlamina to the clay-rich microlamina (×160), (BM6-8; 78–86 cm). d. Transition from a quartz-rich brown lamina to a clay-rich lamina with the occurrence of very thin organic-rich black microlamina (×35) (BM6-5; 36–41 cm).

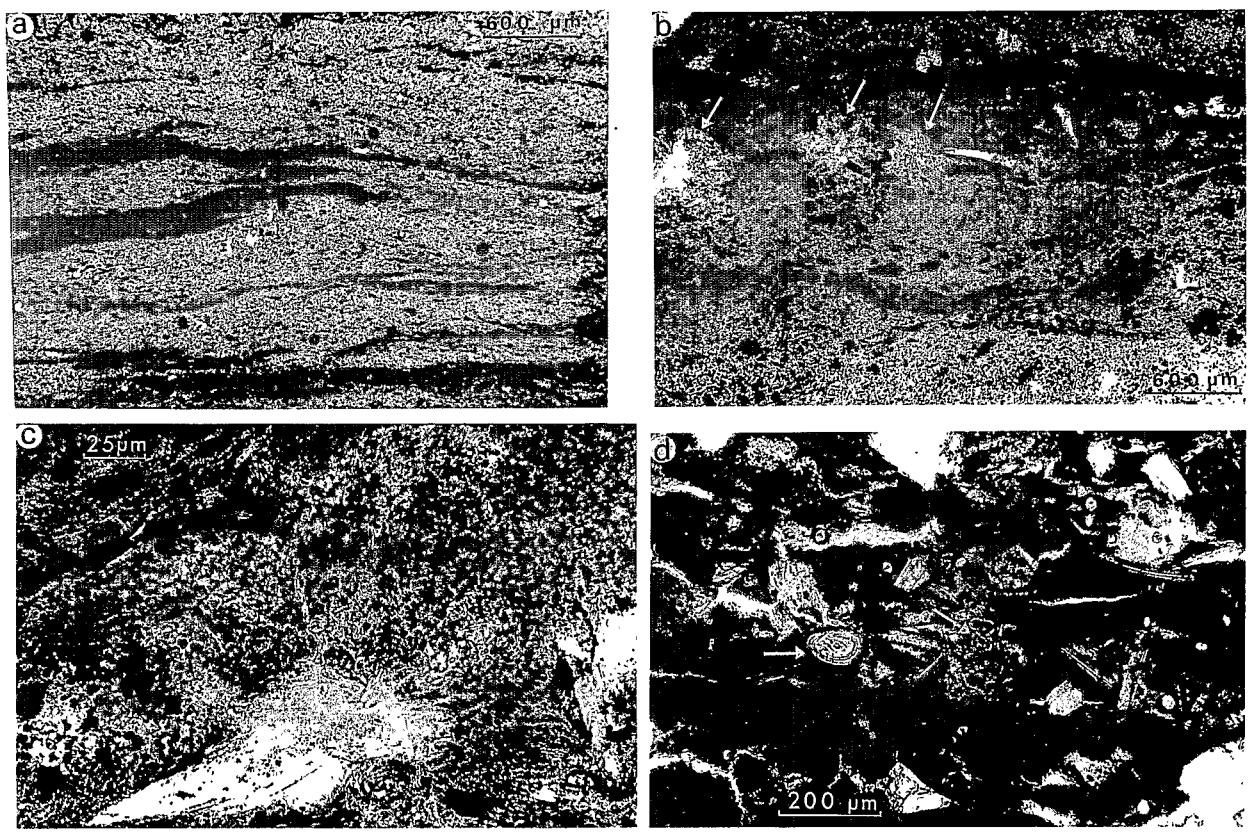

Fig. 13. Thin-section micrograph exhibiting typical sideritic textures. a. Repetition of black microlamina or lenses within clay-rich siderite lamina (x35) (BM6-5; 36–41). b. Alignment of vivianite crystal sprays scattered within a cryptocrystaline sideritic clay-rich lamina (× 35) (BM6-4, 40 cm; BM6-5, 45 cm). c. Detail of vivianite sprays with very fine crystals of siderite lining the periphery (crossed nickels) (×400) (MB6-4; 5–45 cm). d. Pseudo-ooliths or pisoliths of kaolinite and siderite; the cortex consists of siderite and amorphous iron in brown lamina with quartz, sponge spicules and laths of feldspath (×100) (MB6-4, 40 cm; BM6-5, 44 cm)

the exceptional concentrations correspond to visible concretions which recur more commonly in the Pleistocene section. Vivianite which is microscopically obvious, is only noted in a diffractogram as a single subordinate peak. Vivianite occurs most commonly in the older levels of the Pleistocene where values of P_2O_5 contents are two times above the average. Plagioclase feldspar laths are more abundant between 14,000 and 9,000 years BP and correspond to the levels of pyroclastites or influxes from large floods.

Clay mineralogy. In general the clay minerals

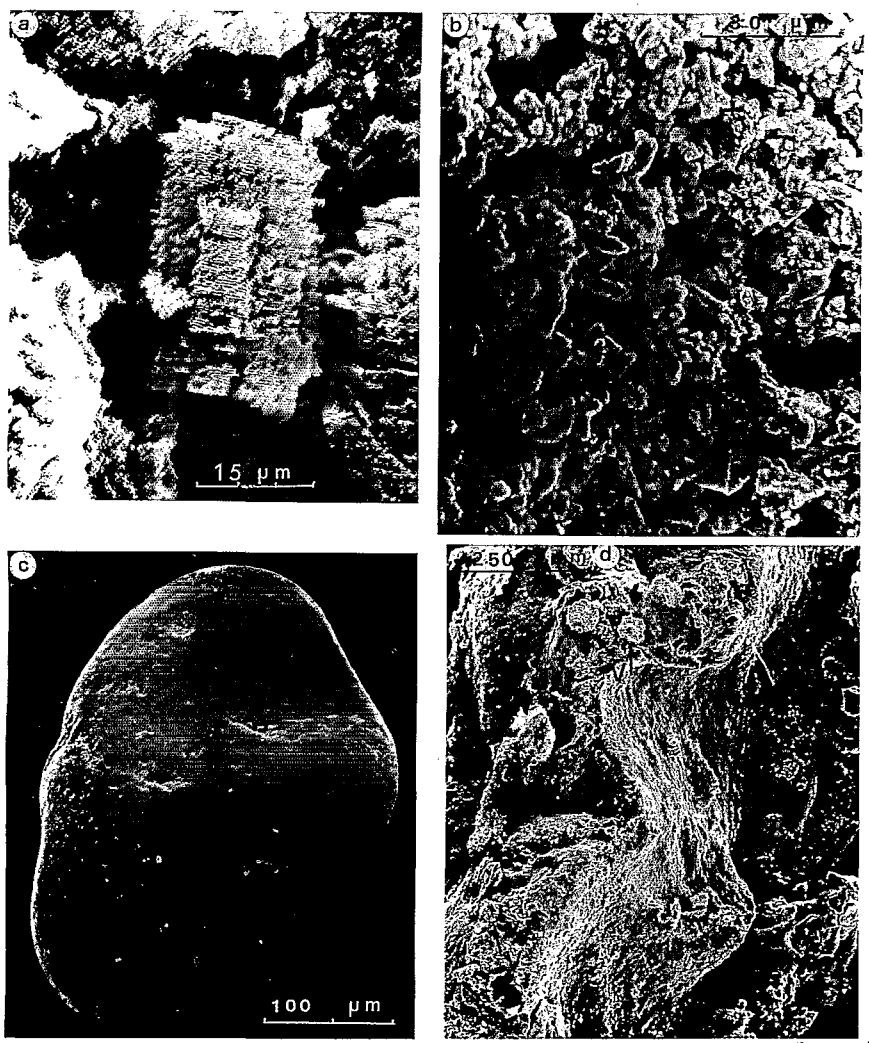

Fig. 14. Scanning electron micrographs from core BM6. a. Concretion of vivianite from a black microlamina (×300) (BM6-2). b. Siderite microcrystal (×1500). c. A ferric-rich clay pellet with indentations on the surface caused by compaction molds from adjoining quartz grains (×300). d. The undulating surface of a microlamina of siderite within a clay-rich lamina; note a surface coating of vivianite (arrows with V), (BM6-5, ×120).

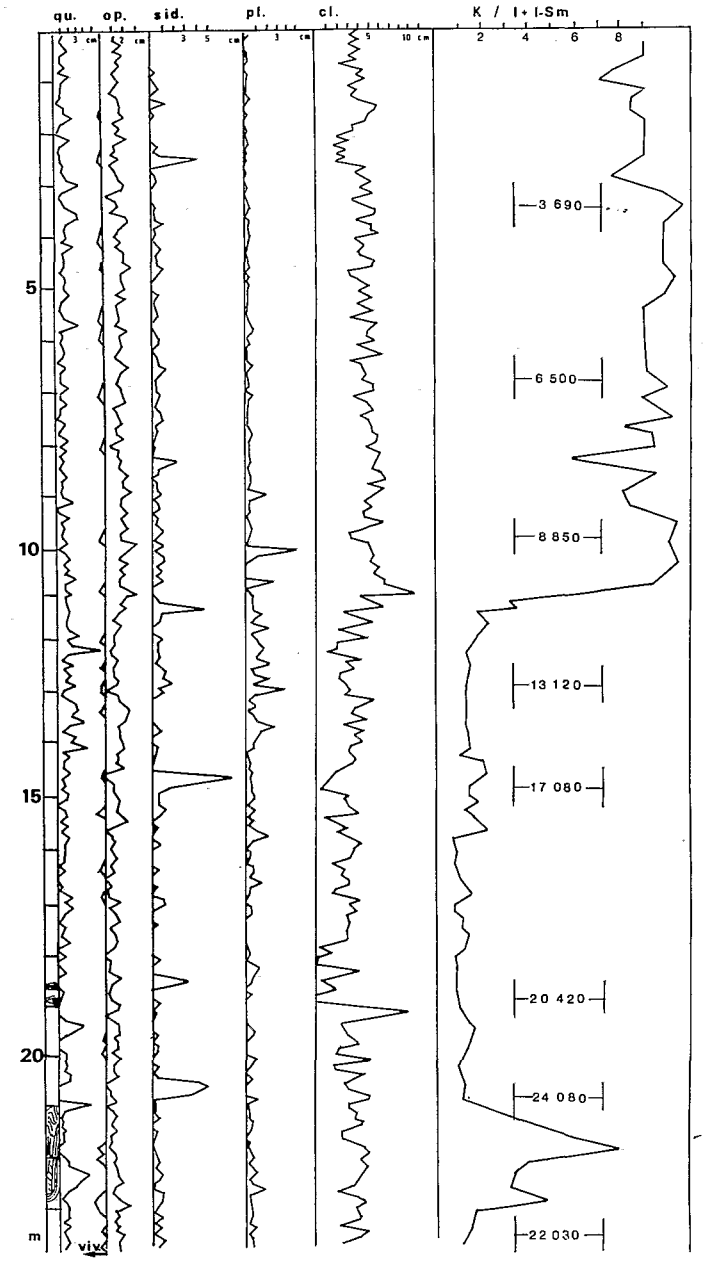

Fig. 15. Log of X-ray diffraction mineralogy based on the maximum relative peak for quartz opal, vivianite, siderite, plagioclastic feldspaths, kaolinite and clays (kaolinite, illite, smectite) according to the relation K/I + I − Sm. The relative intensity of each peak is measured in centimetres.

are most abundant between −12 and −3 m, that is between about 12,000 and 3,000 years BP (Fig. 15). The studies of the size fraction below 2 μm show a general dominance of kaolinite (50 to 90%) associated with illite (10 to 40%) and common traces of mixed layer I–Sm (< 10%). There is no evidence for well-developed pure smectite. The ratio K/I + I − Sm remains near 1 during most of

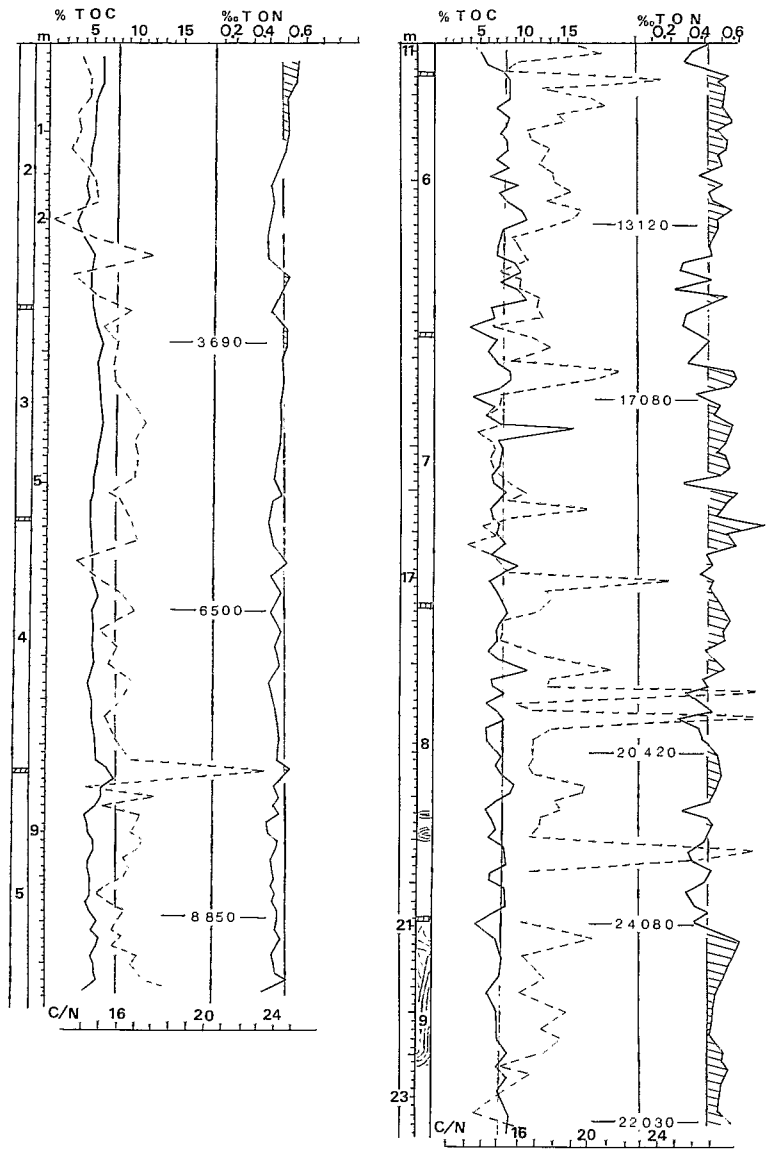

Fig. 16. Log from core BM6 for the values of total organic carbon (TOC) and total nitrogen (TON) and the ratio carbon to nitrogen (C/N).

the Pleistocene and rises suddenly to between 6 and 9 beginning at 12,000 years BP. The ratio diminishes with an irregular slope up to the top of the section. This ratio is also high in the lowermost part of the core which is dated at 26,000 years BP.

Values of total organic carbon around 8% and nitrogen around 0.4% remain fairly constant in the Pleistocene layers (Fig. 16). Organic carbon decreases around −11 m, that is near 10,000 years, and continues at around 5% to the top of the section. Nitrogen follows a parallel curve with values between 0.3 and 0.4 throughout most of the Holocene deposits. There are several levels which may increase to 0.5% or even 0.6%. The ratio C/N is roughly 18 in the Pleistocene deposit, then drops to 15 around 9,000 years and finally to 13 around the second or third last millennium. On the other hand, in detail there are several peaks particularly in the Pleistocene and some in the Holocene where the C/N ratio attains relatively high values above 25. This high ratio commonly corresponds to the presence of brown laminae and particularly of millimetre- to even centimetre-fragments of lignitic debris.

Discussion

Environmental evolution

During the last 20,000 years, sedimentation in Barombi Mbo has been characterized by the accumulation of laminated sediments. One does not observe the varied lithologies found in Lake Bosumtwi, Ghana (Talbot et al., 1984) which include abrupt changes for example to a homogeneous sapropel layer in mid-Holocene, or to diatom-rich layers in the Pleistocene. Core BM6 does not display abrupt changes in the nature of rhythms or detrital input. The basin lacks clear evidence of abrupt or major changes in lake level or evaporites such as occur in the lakes in other less humid zones of Africa (Bosumtwi: Talbot et al., 1984; Tchad: Servant, 1973; Maley, 1981; Bogoria: Tiercelin et al., 1981; Kivu and Tanganyika: Stoffers and Hecky, 1978; Habeyran and Hecky, 1987). In Barombi Mbo the presence of hydromorphic soils and their extension under water provide evidence for lake-level oscillations on the order of metres. If there have been large oscillations during the Quaternary in the level of Barombi Mbo, they have had only a minor effect on the sedimentary balance of the lake. The pollen spectrum (Brenac, 1988) documents the continuous presence of aquatic plants showing the presence of a perennial lake. Low levels were infrequent and high levels would be controlled by outlet overflow.

Palynologic studies (Maley and Brenac, 1987; Brenac, 1988; Maley, 1989) indicate that the percentages of graminae pollen remain relatively low all along the core BM6 (0–25%, with 7% today). This result implies a long-term forest cover in the Barombi Mbo region which may have played a role as a refuge. In spite of this persistence, the ecosystem shows significant fluctuations corresponding to climatic changes. Between 24,000 to 20,000 years BP the abundance of forest and montane-type plants suggests a more humid and cooler environment than today; from 20,000 to 15,000 years BP an increase in the total herbaceous pollen implies a relatively dry and cool climate; beginning 14,000 years BP, the semi-deciduous forest developed with several pioneer forest taxa. The climate returned to higher humidity but with warmer climate than before 20,000 years BP.

Flux of particulate material

The sedimentary deposits derived from the Toh Mbok stream, defined a classic, small prograding delta and delta slope with a uniform slope which extends to the basin plain, contrasting distinctly with the other shores (Kelts et al., 1986). Grain sizes show a lateral change from very silty-rich with coarse fragments of land-derived organic debris becoming progressively finer towards the basin plain and thereby accumulating exclusively as laminae. The overall frequency of repetition of these laminae which appears to be about 1 per 15.4 years throughout the section, is interpreted to define the order of magnitude of the recurrence

rate for large flood events in this intertropical African zone. Such frequencies have been registered in secular variations from Senegal (Gac et al., 1983), Nigeria (Nedeco, 1961), Congo (Kinga-Mouzeo, 1986). Links with a solar cycle remain as yet uncertain (Herman and Goldberg, 1978). Flood events are represented in the sediment by the occurrence of coarser-grained brown microlaminae at the base of microsequences. Grey laminae in the upper part of a microsequence are interpreted as the slow decantation of clayey organic-rich matter from suspension, as well as the fine-grained influxes of the following years. During intervening periods the flood deposits are documented by darker microlaminae of silt and organic matter which form the first step of a new microsequence.

Interaction of these processes shows that the chronological fluctuations which are controlled by the climatic oscillations, are possibly to analyse in the core BM6.

(1) During the period 20,000 to 14,000 years BP, the sedimentation rate is lowest because precipitation becomes less abundant and floods less frequent but more forceful as shown by the brown laminae which are thicker and relatively coarser. Soils in the drainage basin became dominated particularly by mica-family minerals, which comprise more than half of the spectrum.

(2) Beginning around 14,000 years BP and certainly since 12,000 BP and continuing throughout the Holocene there is a distinct increase in the rate of deposition (> 40 g cm^{-2} 10^3 yrs) but also a reduction in the apparent frequency of the brown laminae. Inflow suspensions became more important but also more uniform; the brown laminae became less thick or absent over several decimetres. Under these conditions, the turbid inflows are marked simply by the intercalation of brown *microlaminae*, less than 1 mm thick, within clayey sublaminae. Some of these inflows may indicate significant increases in seasonal precipitation if the vegetation remained lush. During phases of generally higher humidity, soil development in the drainage basin was more intensive and favoured the formation of kaolinite which is 6 times more abundant in the clay spectrum than illite–smectite types.

Hydrodynamics of sedimentation

Each of the laminae corresponds to a more or less abrupt input of alluvial matter from within the limited catchment with its short transport pathways. Some of the basinal layers derive from episodic stripping of thin deposits plastered on the crater's low terraces near the river mouth and also from beaches and littoral habitats of 2–3 m maximum depth, particularly those containing a bio-assemblage with shallow-water sponge spicules. Much of the 2 km in diameter surface of the lake becomes clouded and decants its suspension progressively by grain-size settling to form the characteristic laminations.

River plumes seem a major depositional mechanism for restricted basins such as Barombi Mbo. Particulate material gradually settles, well-sorted quartz grains first, which are followed by laths of plagioclase, mica flakes, coarser organic debris and sponge spicules (resuspended by storms). Thus a lower sublamina lacks clay particles which are common in the basal parts of a slump-generated turbidite (e.g., Bouma, 1962).

River-plume input is the most important sediment transport mechanism in many small lakes such as Kamloops Lake (Pharo and Carmack, 1979), Cayuga Lake (Ludlam, 1967), Vänern Lake (Håkanson and Jansson, 1983). In Barombi Mbo, episodic turbidity currents derived from floodwater underflows occur, particularly in beds before 12,000 years BP, where upper sublaminae commonly contain coarse particles.

The sediment evidence suggests that turbidites are less important to overall sedimentation: coarse grains greater than 200 μm are absent in deposits below 110 m water depth, but occur in deltaic sediments. Deepwater laminae do not show truncation or density current erosion features. Depending on conditions associated with sudden floods, episodic density interflows or underflows are likely.

Organic inputs to the lake system

A stable stratification and an anoxic interface near the lake surface, limits seasonal recycling of nutrients into the epilimnion. Plankton productivity is therefore relatively low in Barombi Mbo, and land-derived organic matter dominates over the aqueous type. C/N ratios support this conclusion because the plot remains fairly uniform throughout the Quaternary sections recovered, with the exception of coarse-grained layers which have macroscopic lignin fragments. A gradual increase in C/N ratio from 13 to 18 is explained as a result of progressive degradation processes during diagenesis, which selectively attack nitrogen compounds such as amino-acids.

Shifts in the composition of organic matter may also be explained by an increase in the debris from C3-type plants, mainly trees which are rich in cellulose, during the Holocene concomitant with the demise of the C4-type plants such as the grasses. The $\delta^{13}C$ values of Pleistocene organic matter are on the order of -31 and -34‰, whereas those from the first levels of the Holocene range around -23 to -27‰ (measurements of Hillaire-Marcel, in prep.).

The apparent low productivity of the biomass in the epilimnion is suggested by a nearly total absence of diatom frustules in the deposits with the exception of a few levels around 20,000 years BP. In these levels rare frustules persist along with faecal pellets from undetermined limnivorus organisms. Associated organic matter is more of the exinite- than the alginite-type. Finally the lack of any evidence for significant fluctuations in lake levels suggests that the pattern of organic matter production and oxidation did not change much during the drier interval from 15,000 to 20,000 years BP.

CO_2 gas

Reconnaissance seismic profiling surveys of the bottom of Barombi Mbo using a 3.5 kHz system showed limited penetration to about 6–10 m partly due to exsolved gases. Beneath a parallel-stratified, transparent zone of about 6–10 m, seismic energy is absorbed along an irregular surface which was interpreted as the result of slumping along the outer slope apron of the lake (Kelts et al., 1986). The deformation observed in sediment cores below 18.6 m cannot derive from transport from upper slope areas. The basic character and the grain sizes of the disturbed sediments match the sediment facies in basinal areas and are distinct from those of the slopes and the deltaic region. The preservation of laminated slabs implies that transport distances were limited, and did not destroy all primary bedding. One most likely causal mechanism is thought to derive from earthquake creep due to nearby volcanic activity.

An alternative explanation for the disturbed section with tilted lamination sets, could be related to localized bursts of phreatic gases. Gases occur in the top metres of some of the cores recovered (Maley et al., 1990), and are also suggested by the character of the seismic records (Kelts et al., 1986). Although this mechanism appears unlikely from the extent of the features in seismic profiles, it must be considered in the light of recent tragedies at nearby lakes Nyos and Monoum (Conference of Yaoundé, 1987, see Sigvaldason, 1989). Magmatically derived CO_2 gas has been proven in those lakes, although the mechanism for emissions remains controversial. One explanation favours slow build-up to supersaturation and spontaneous gas bursts from the lake waters (Sigurdsson et al., 1987; Kling et al., 1987). The opposing hypothesis favours a sudden expulsion of CO_2 trapped in the volcanic pipe breccia below (Barberi et al., 1989; Tazieff, 1989). If the disturbed sections in Lake Barombi Mbo sediments are related to gas expulsion from below the lake floor around 20,000 years BP, then this would add support for the second hypothesis. Further data are needed to document the extent and form of these pre-20,000 year BP disturbances.

Conditions for siderite precipitation

Siderite is the only primary carbonate mineral found in the cored sediment. Kling (1987) reported rhodochrosite associated with siderite from one of the clay microlaminae, but this could not be substantiated from any of the different fractions (bulk sediment, microlaminae portions, or concretions), or in any of the size fractions. On the other hand, levels of MnO up to 2–5% in some layers of the Pleistocene sediment, suggest a possibility for rhodochrosite formation.

The formation of siderite within the pore waters near to the sediment–water interface is favoured by a number of factors which increase the concentration of Fe^{2+} or CO_3^{2-}. These include break-down of organic matter in the hypolimnion, then post-depositional degradation of organic matter and release of CO_2 as indicated by profiles of C/N. An acidification of the environment favours the dissolution of oxides and hydroxy ferric-oxides derived from weathering products of the volcanic terrane. Finally iron may be released and associated with organic acids (Lundgren and Dean, 1979). The formation of siderite requires not only an environment with very low redox potentials but also very low concentrations of sulfur and thus low fluxes of sulfate, or else pyrite may form. Kling (1987) reports that the concentration of sulfate near the surface is extremely low (0.20 mg/l) and negligible near to the bottom (less than 0.02 mg/l). This contrasts with Lake Nyos where active hydrothermal vents inject waters richer in sulfate and have thus promoted the formation of pyrite with siderite near the bottom (Bernard and Symonds, 1989).

According to Berner (1971), the formation of iron-carbonates instead of calcium carbonate indicates ratios of Fe/Ca greater than 0.05. If the concentration of calcium in solution is estimated between 2 and 3% then iron in solution is difficult to determine due to the presence of micro-colloids which persist even after filtration at 0.12 mm. It has been shown for the oceanic plume from the Congo–Zaire River (Figuères et al., 1978), having a pH of 6 to 7.7, that pseudo-solutions of iron persist even after the use of successive filters with very fine pores or even down to ultra-centrifugation. In Barombi Mbo, iron in solution (Fe^{2+}) is practically negligible below 100 m depth. The pH values from 6.42 to 6.47 (Kling, 1987) are too high. It is thus possible to precipitate siderite in the hypolimnion waters near to the sediment–water interface although it seems more likely that the pH of interstitial waters provides a better microenvironment for the formation of this mineral. The hydrological data of Kling (1987) do not report the presence of siderite crystals from any of the suspended matter samples taken from any part of the water column. Microcrystals of siderite are more or less disseminated within the microlaminae of clay, but also occur as microlaminations which seem to document short interface episodes more favourable to their precipitation. These zones appear related to slower sedimentation rates; siderite is lacking in the brown laminae as well as in the pro-deltaic deposits. The siderite concretions which display a cloudy diffuse character reflect the micro-porosity of the sediment, and their irregular occurrences imply post-depositional nucleation processes. Finally, the yellow concretions confined to the Pleistocene layers which commonly deform sedimentary structure, imply diagenetic crystallization processes.

The close relationship of siderite formation to methanogenesis may be explained by the rate of microbial organic matter degradation, which governed both methanogenesis (Talbot and Kelts, 1986) and CO_2 availability (Bahrig, 1989). CO_2 can be supplied from several distinct sources such as volcanic gas (Bahrig, 1988) or microbial activity (Hangari et al., 1980), although the presence of magmatic CO_2 in Barombi Mbo has yet to be confirmed by isotopic analyses.

Spherolitic crystals of vivianite accompany the clayey and the most organic-rich laminae as typical diagenetic products (Jakobsen, 1988). We assume that alkaline basalts in the drainage basin are rich in phosphorus. Vivianite is commonly found together with siderite. Equilibrium calculations (Nriagu, 1972; Nriagu and Dell, 1974) show that, except for high concentrations of dissolved phosphate, the conditions for the formation of vivianite are similar to those for siderite.

Finally we note that there was no evidence of diagenesis in the abundant pyroclastic particles. Rare grains of iddingsite derive from subareal weathering processes.

Conclusions

In contrast with numerous previously studied African lakes, Lake Barombi Mbo persisted in the intertropical environment with a relatively stable water level throughout the late Pleistocene and Holocene period. The deposits show no clear evidence of evaporative concentration, desiccation or oxidation which would suggest major level changes. It is only the relatively sudden variations in sedimentation rates, amounts of organic matter and diatom, the frequency of laminations and the clay-mineral assemblages which provide evidence of relative changes in either climate or the nature of the vegetation cover of the drainage basin.

The permanent stratification of the lake has promoted the accumulation of organic-matter-rich sediments although the organic matter is derived mainly from terrigenous sources (exinite). The productivity of planktonic biomass has remained limited. Early diagenetic processes combined CO_2 released from organic matter degradation (and possibly additional magmatic CO_2) with iron in solution delivered by the weathering of the soils in the catchment basin in order to form siderite. Availability of Fe^{2+} at the base of the hypolimnion seems less related to anoxia than due the higher pH conditions.

Among the different sedimentary processes recently inventoried for small lakes by Hilton et al. (1986), Barombi Mbo exhibits a delta with a prograding slope where the coarser particles settle during the dissipation of the influx energy. Sedimentation is gradual from fluvial plumes or density underflows. Laminated deposits occur deeper than 90 m in waters undisturbed by wind-generated currents. But, due to wind action or river swell, the continuous or intermittent reworking phenomena are unlikely.

The sedimentation patterns in core BM6 suggest that the Lake Barombi Mbo region has not experienced a drastic change in hydrological character since before the last glacial maximum. The character of the sediments also suggests no major volcanic activity or gas events within the last 20,000 years.

Acknowledgements

This research was undertaken with support from ORSTOM program GEOCIT, the CNRS and the NSF and was sponsored by the Ministry of Higher Education and Research of Cameroon. Special thanks are due to D.A. Livingstone and his crew who managed the coring operations. During opening and subsampling of the cores at ORSTOM (Bondy, France) technical assistance of Mrs. J. Harlé and M. Delaune was greatly appreciated. The authors are also grateful to M. Fournier (ORSTOM, Bondy) for the radiocarbon dates and to E. Gavinelli and C. Riandey (ORSTOM, Bondy) for many analyses. Thanks are also due to M. Talbot and J.J. Tiercelin for reviewing earlier versions of this manuscript and providing many useful comments for its improvement. K. Kelts acknowledges support from a research grant of the ETH-Zürich and the field assistance of M. Haag.

References

Bahrig, B., 1988. Paleoenvironment information from deep water siderite (Lake of Laach, W Germany) In A. Fleet, K. Kelts and M. Talbot (Editors), Lacustrine Petroleum Source Rocks. Geol. Soc. London, Spec. Publ., 40: 153–158.

Bahrig, B., 1989. Stable isotope composition of siderite as an indicator of the paleoenvironmental history of oil shale lakes. Palaeogeogr., Palaeoclimatol., Palaeoecol., 70: 139–151.

Barberi, F., Chelini, W., Marinelli, G. and Martini, M., 1989. The gas cloud of Lake Nyos (Cameroun, 1986): results of the Italian Technical Mission. J. Volcanol. Geotherm. Res., 39: 125–134.

Bernard, A. and Symonds, R.B., 1989. The significance of siderite in the sediments from Lake Nyos, Cameroon J. Volcanol. Geotherm. Res., 39: 187–194.

Berner, R.A., 1971. Chemical Sedimentology. McGraw-Hill, New York, N.Y., 240 pp.

Bongo-Passi, G., Gadel, F., Giresse, P., Kinga-Mouzeo and Moguedet, G., 1988. Séquences géochimiques et minéralogiques dans l'éventail détritique profond quaternaire du fleuve Congo à 2000 m et 4000 m de fond; sédimentogenèse et diagenèse. Bull. Soc. Géol. Fr., (8), 4: 437–452

Bouma, A.H., 1962. Sedimentology of Some Flysch Deposits Elsevier, Amsterdam, 168 pp.

Brenac, P., 1988. Evolution de la végétation et du climat dans l'Ouest-Cameroun entre 25,000 et 11,000 ans BP Inst. Fr. Pondichéry, Trav. Sec. Sci. Tech., 25: 91–103.

Cornaccia, M. and Dars, R., 1983. Un trait structural majeur du continent africain. Les linéaments centrafricains du Cameroun au Golfe d'Aden. Bull. Soc. Géol. Fr., (7), 25: 101–109.

Dumort, J.C., 1968. Carte Géologique et Notice explicative Feuille Douala-Ouest. Dir. Mines et Géologie Cameroun. Bureau Rech. Géol. et Minières, Paris, 69 pp.

Figuères, G., Martin, J.M. and Meybeck, M., 1978 Iron behaviour in the Zaire estuary. Neth. J. Sea Res., 12: 329–337

Fitton, J.G. and Dunlop, H.M., 1985. The Cameroon Line, West Africa and its bearing on the origin of oceanic and continental alkali basalts. Earth Planet. Sci. Lett., 72: 23–28.

Gac, J.Y., Monteillet, J. and Faure, H., 1983. Marine shoreline in estuaries as palaeoprecipitations indicators In: A

Street-Perrot and al. (Editors), Variations in the Global Water Budget. Reidel, Dordrecht, pp. 361–370.

Gèze, B., 1943. Géographie physique et géologie du Cameroun occidental. Mem. Mus. Nat. Hist. Nat., Paris, 17, 272 pp.

Green, J., Corbet, S.A. and Betney, E., 1973. Ecological studies on crater lakes in West Cameroon. The blood of endemic Cichlids in Barombi Mbo in relation to stratification and their feeding habits. J. Zool. London, 170: 299–308.

Haberyan, K.A. and Hecky, R.E., 1987. The Late Pleistocene and Holocene stratigraphy of lakes Kivu and Tanganyika. Palaeogeogr., Palaeoclimatol., Palaeoecol., 61: 169–197.

Håkanson, J. and Jansson, M., 1983. Principles of Lake Sedimentology. Springer Verlag, Berlin, 280 pp.

Hangari, K.M., Ahmad, S.N. and Perry, E.C., 1980. Carbon and oxygen isotopes ratios in diagenetic siderite and magnetite from Upper Devonian Ironstone, Wadi Shatti District, Libya. Econ. Geol., 75: 538–545.

Hassert, K., 1912. Seenstudien in Nord-Kamerun. Z. Ges. Erdkd., Berlin, pp. 7–41; 135–144; 203–216.

Herman, J.R. and Goldberg, R.A., 1978. Sun, Weather and Climate. NASA Publ., SP-426, Washington, D.C., 360 pp.

Hilton, J., Lishman, J.P. and Allen, P.V., 1986. The dominant processes of sediment distribution and focusing in a small, eutrophic, monomictic lake. Limnol. Oceanogr., 31: 125–133.

Jakobsen, B.H., 1988. Accumulation of pyrite and Fe-rich carbonate and phosphate minerals in a lowland moor area. J. Soil Sci., 39: 447–455.

Kinga-Mouzeo, 1986. Transport particulaire actuel du fleuve Congo et de quelques affluents; enregistrement quaternaire dans l'éventail détritique profond (sédimentologie, minéralogie et géochimie). Thèse Doct., Univ. Perpignan, 251 pp.

Kelts, K., Haag, M. and Maley, J., 1986. Subottom profiling in Cameroon crater lakes. Rep. ETH/EAWAG, Zürich (Manuscript, 15 pp).

Kling, G.W., 1987. Comparative Limnology of Lakes in Cameroon, West Africa. Ph. D. thesis, Duke University, 482 pp.

Kling, G.W., 1988. Comparative transparency, depth of mixing, and stability of stratification in lakes of Cameroon, West Africa. Limnol. Oceanogr., 33: 27–40.

Kling, G.W., Clark, M.A., Comton, H.R., Devine, J.D., Eevans, W.C., Humpgrey, A.M., Koenigsberg, E.J., Lockwood, J.P., Tuttle, M.L. and Wagner, G.N., 1987. The 1986 lake Nyos gas disaster in Cameroun, West Africa. Science, 236: 169–175.

Kranck, K., 1984. Grain size characteristics of turbidite. In: D.A.V. Stow and D.J.W. Piper (Editors), Fine-Grained Sediments: Deep Water Processes and Facies. Blackwell, Oxford, pp. 83–92.

Letouzey, R., 1968. Etude phytogéographique du Cameroun. P. Lechevalier, Paris, 508 pp.

Letouzey, R., 1985. Notice de la carte phytogéographique du Cameroun au 1/500.000è. Inst. Rech. Agron., Yaoundé et Inst. Carte Intern. Vég., Toulouse.

Lockwood, J.P. and Rubin, M., 1989. Origin and age of the Lake Nyos maar, Cameroon. J. Volcanol. Geotherm. Res., 39: 117–124.

Ludam, S.D., 1967. Sedimentation in Cayuga Lake, New York. Limnol. Oceanogr., 12: 618–632.

Lundgren, D.G. and Dean, W., 1979. Biogeochemistry of iron. In: P.A. Trudinger and D.Y.Swaine (Editors), Biogeochemical Cycling of Mineral-Forming Elements. Elsevier, Amsterdam, pp. 211–251.

Maley, J., 1981. Etudes palynologiques dans le bassin du Tchad et paléoclimatologie de l'Afrique nord-tropicale de 30.000 ans à l'époque actuelle. Trav. Doc. O.R.S.T.O.M., Paris, 219, 586 pp.

Maley, J., 1987. Fragmentation de la forêt dense humide africaine et extension des biotopes montagnards au Quaternaire récent: nouvelles données polliniques et chronologiques. Implications paléoclimatiques et biogéographiques. Palaeoecol. Afr., 18: 307–334.

Maley, J., 1989. Quaternary climatic changes in the African rain forest: forest refugia and the major role of sea surface temperature variations. In: M. Leinen and M. Sarnthein (Editors), Paleoclimatology and Paleometeorology: Modern and Past Patterns of Global Atmospheric Transport. Kluwer, NATO Adv. Sci. Inst., Ser. C, Math. Phys. Sci., 282: 585–616.

Maley, J. and Brenac, P., 1987. Analyses polliniques préliminaires du Quaternaire récent de l'Ouest-Cameroun: mise en évidence de refuges forestiers et discussion des problèmes paléoclimatiques. Mém. Trav. E.P.H.E., Inst. Montpellier, 17: 129–142.

Maley, J., Livingstone, D.A., Giresse, P., Thouveny, N., Brenac, P., Kelts, K., Kling, G., Stager, C., Haag, M., Fournier, M., Bandet, Y., Williamson, D. and Zogning, A., 1990. Lithostratigraphy, volcanism, paleomagnetism and palynology of Quaternary deposits from Barombi Mbo (West-Cameroon): preliminary results. J. Volcanol. Geotherm. Res., 42: 319–335.

Nedeco (Netherlands Engineering Consultants), 1969. River Studies and Recommendation on Improvement of Niger and Bénoué. North Holland Publishing Co., Amsterdam, 111 pp.

Nriagu, J.O., 1972. Stability of vivianite and ion-pair formation in the system $Fe(PO_4)^{2-}$ $H_3PO_4^-$, H_2O. Geochim. Cosmochim. Acta, 36: 459–470.

Nriagu, J.O. and Dell, C.J., 1974. Diagenetic formation of iron phosphates in recent lake sediments. Am. Mineral., 59: 934–946.

Pharao, C.H. and Carmack, E.C., 1979. Sedimentation processes in a short residence-time inter montane lake, Kamloops Lake, British Columbia. Sedimentology, 26: 523–541.

Richards, P.W., 1963. Ecological notes on West African vegetation, II. Lowland forest of the Southern Bakundu Forest Reserve. J. Ecol., 51: 123–149.

Rivière, A., 1952. Sur la représentation graphique de la granulométrie des sédiments meubles. Bull. Soc. Géol. Fr., (6), 2: 145–154.

Servant, M., 1973. Séquences continentales et variations climatiques. Evolution du Bassin du Tchad au Cénozoïque supérieur. Thèse Sc., Paris, Trav. Doc. O.R.S.T.O.M. Paris, (1984), 159, 573 pp.

Sigurdsson, H., Devine, J.D., Tchoua, F.M., Presser, T.S., Pringle, M.K. and Eevans, W.C., 1987. Origin of the lethal gas burst from Lake Monoum, Cameroun. J. Volcanol. Geotherm. Res., 31: 1–16.

Sigvaldason, G.E., 1989. International Conference on Lake Nyos disaster: conclusions and recommendations. J. Volcanol. Geotherm. Res., 39: 97–108.

Stoffers, P. and Hecky, R.E., 1978. Late Pleistocene–Holocene evolution of the Kivu–Tanganyika Basin. In: A. Matter and M.E. Tucker (Editors), Modern and Ancient Lake Sediments. Int. Assoc. Sedimentol., Spec. Publ., 2: 43–55

Suchel, J.B., 1972. La répartition des pluies et les régimes pluviométriques au Cameroun. Trav. Doc. Géogr. Trop., C.E.G.E.T., Bordeaux, 5: 287 pp.

Suchel, J.B., 1988. Les climats du Cameroun. Thèse Sc., Saint Etienne, 4 t.

Talbot, M.R. and Kelts, K., 1986. Primary and diagenetic carbonates in the anoxic sediments of Lake Bosumtwi, Ghana. Geology, 14: 912–916.

Talbot, M.R., Livingstone, D.A., Palmer, P.G., Maley, J., Melack, M.J., Delibrias, G. and Gulliksen, S., 1984. Preliminary results from sediment cores from Lake Bosumtwi, Ghana. Palaeoecol. Afr., 16: 173–192.

Tazieff, H., 1989. Mechanisms of the Nyos carbon dioxide disaster and of so-called phreatic steam eruption. J. Volcanol. Geotherm. Res., 39: 109–116.

Thouveny, N. and Williamson, D., 1988. Palaeomagnetic study of the Holocene and Upper Pleistocene sediments from Lake Barombi Mbo, Cameroon: first results. Phys. Earth Planet. Inter., 52: 193–206

Tiercelin, J.J., Mondeguer, A., Gasse, F., Hillaire-Marcel, C., Hoffert, M., Larque, P., Ledee, V., Marestang, P., Ravenne, C., Raynaud, J.F., Thouveny, N., Vincens, A. and Williamson, D., 1988. 25.000 ans d'histoire hydrologique et sédimentaire du lac Tanganyika, Rift Est-africain. C.R. Acad. Sci., Paris, II, 307: 1375–1382.